Available online at www.sciencedirect.com

SciVerse ScienceDirect

Ceramics International 39 (2013) 7467–7474

CERAMICS INTERNATIONAL

www.elsevier.com/locate/ceramint

Structural studies of porous Ni/YSZ cermets fabricated by the solid-state reaction method

J. Kim[a], K.H. Cho[b], I. Kagomiya[c], K. Park[a,*]

[a]*Faculty of Nanotechnology and Advanced Materials Engineering, Sejong University, Seoul 143-747, Republic of Korea*
[b]*R&D Center, Samchun Pure Chemical Co., Pyeongtaek-si, Gyeonggi-do 440-3, Republic of Korea*
[c]*Materials Science and Engineering, Nagoya Institute of Technology, Nagoya 466-8555, Japan*

Received 21 December 2012; received in revised form 29 January 2013; accepted 27 February 2013
Available online 14 March 2013

Abstract

Carbon black-added NiO/YSZ composites exhibited a highly porous structure due to the enhanced evolution of CO and CO_2 gases associated with exothermic reactions during sintering. The addition of carbon black resulted in a decrease in the density and grain size of NiO/YSZ composites. The porosity of NiO/YSZ composites increased with decreasing the sintering temperature and increasing the NiO content. Additionally, highly porous Ni/YSZ cermets were fabricated by reducing the NiO/YSZ composites in ($Ar+6\%\ H_2$), which was attributed to the change of NiO to Ni and then the extraction of oxygen. The carbon black used as a pore-former was highly effective for preparing porous Ni/YSZ cermets.

Keywords: A. Powders: solid state reaction; A. Sintering; B. Microstructure-final; B. Porosity

1. Introduction

Solid oxide fuel cells (SOFCs) are solid-state electrochemical devices that convert chemical energy in fuels directly into electricity [1–4]. Recently, SOFCs have received significant attention due to high conversion efficiency, low pollution emission, high flexibility to various fuels (H_2, CH_4, etc), and the need for green technologies against climate change [1,5]. Ni/yttria stabilized zirconia (YSZ) cermets are generally utilized as the anode and anode functional layer in SOFC [6]. Ni acts as a catalyst owing to its relatively high electrocatalytic activity of H_2 oxidation, low cost, and high chemical stability at high temperatures. YSZ constitutes a framework for the dispersion of Ni particles, allows for a porous structure, suppresses the grain growth of Ni particles during the reduction of NiO/YSZ composites and the operation at high temperatures, and provides the thermal expansion coefficient of the cermets acceptably close to that of other cell components [6–9]. In addition, it plays an important role of ionic contribution to the overall conductivity and broadens the triple phase boundary (TPB), which consists of anode, electrolyte, and pore for reaction gas.

Since the electrochemical performance of Ni/YSZ cermets depends strongly on the microstructure and Ni content, considerable efforts have been made for the precise control of the microstructure and Ni content [10]. Sufficient porosity is necessary for the diffusion of large amounts of fuel and reaction products during operation at high current densities. It is known that controlling the process, especially sintering, is a promising route for improving the structural and electrical characteristics. Therefore, in the present work, we sintered NiO/YSZ green pellets at various temperatures (1250–1400 °C). Pore-formers such as flour and rice starch were used for creating porous structures [8,11]. Here carbon black as a pore-former is utilized. We investigated the effect of carbon black, the sintering temperature, and the Ni content on the structural properties of Ni/YSZ cermets. In order to maximize the performance, appropriate carbon black content as well as appropriate sintering and reduction schemes are needed.

---

[*] Corresponding author. Tel.: +82 2 3408 3777; fax: +82 2 3408 4342.
E-mail address: kspark@sejong.ac.kr (K. Park).

0272-8842/$ - see front matter © 2013 Elsevier Ltd and Techna Group S.r.l. All rights reserved.
http://dx.doi.org/10.1016/j.ceramint.2013.02.094

2. Experimental

The following commercially available powders were used as starting raw materials: (1) NiO (99.97%; Kojundo Chemical Co.), (2) yttria-stabilized zirconia (8YSZ; Tosoh Co.), and (3) carbon black (Alfa Aesar Johnson Matthey Co.). The NiO, YSZ, and carbon black powders were weighed in appropriate proportions (Table 1). For each composition, the powders were mixed with ethanol for 5 h at 350 rpm using a planetary mill (Fritsch Pulverisette 6) and ZrO_2 balls. The mixture was dried at 60 °C in an oven for 24 h. The dried powders were then carefully ground in mortar and passed through a 100-mesh sieve. Subsequently, the sieved powders were pressed at a uniaxial pressure of 62 MPa to prepare green pellets of 3 mm-thick and 10-mm in diameter. The green pellets were heated at 1250–1400 °C for 3 h in air and then furnace cooled. The sintered NiO/YSZ composites were reduced at 1000 °C in (Ar+6% H_2) atmosphere for 3 h to form Ni/YSZ cermets. The crystal structure of the NiO/YSZ composites and Ni/YSZ cermets was analyzed with an X-ray diffractometer (XRD; Rigaku DMAX-2500) using Cu Kα radiation at 40 kV and 100 mA. The microstructure of the fabricated samples was investigated with a field emission scanning electron microscope (FE-SEM; Hitachi S-4700). The bulk density of the samples was measured by the Archimedes method.

Table 1
Chemical composition of the NiO/YSZ composites designed in this study.

Sample	Composition (wt%)
Sample 30A	NiO:YSZ=30:70
Sample 40A	NiO:YSZ=40:60
Sample 50A	NiO:YSZ=50:50
Sample 60A	NiO:YSZ=60:40
Sample 30B	NiO:YSZ:C*=30:70:5
Sample 40B	NiO:YSZ:C*=40:60:5
Sample 50B	NiO:YSZ:C*=50:50:5
Sample 60B	NiO:YSZ:C*=60:40:5
Sample 30C	NiO:YSZ:C*=30:70:10
Sample 40C	NiO:YSZ:C*=40:60:10
Sample 50C	NiO:YSZ:C*=50:50:10
Sample 60C	NiO:YSZ:C*=60:40:10

C* indicates carbon black.

3. Results and discussion

Fig. 1(a), (b), (c) and (d) shows the XRD patterns of the NiO/YSZ composites (5 wt% carbon black) sintered at 1250, 1300, 1350, and 1400 °C, respectively. The NiO/YSZ composites contain two crystalline phases, i.e., the NiO with a cubic structure and the YSZ with a cubic structure [12,13]. No second phases or impurities are present. It has been reported that NiO is dissolved in 8YSZ by a highly limited amount [14]. The solubility of NiO in 8YSZ is below 5 mol%. The NiO dissolution in 8YSZ stabilizes the cubic 8YSZ phase at high temperatures [15]. As expected, by increasing the NiO content in the composites, the intensity of NiO peaks is increased, while the intensity of YSZ peaks is decreased. The added carbon black and

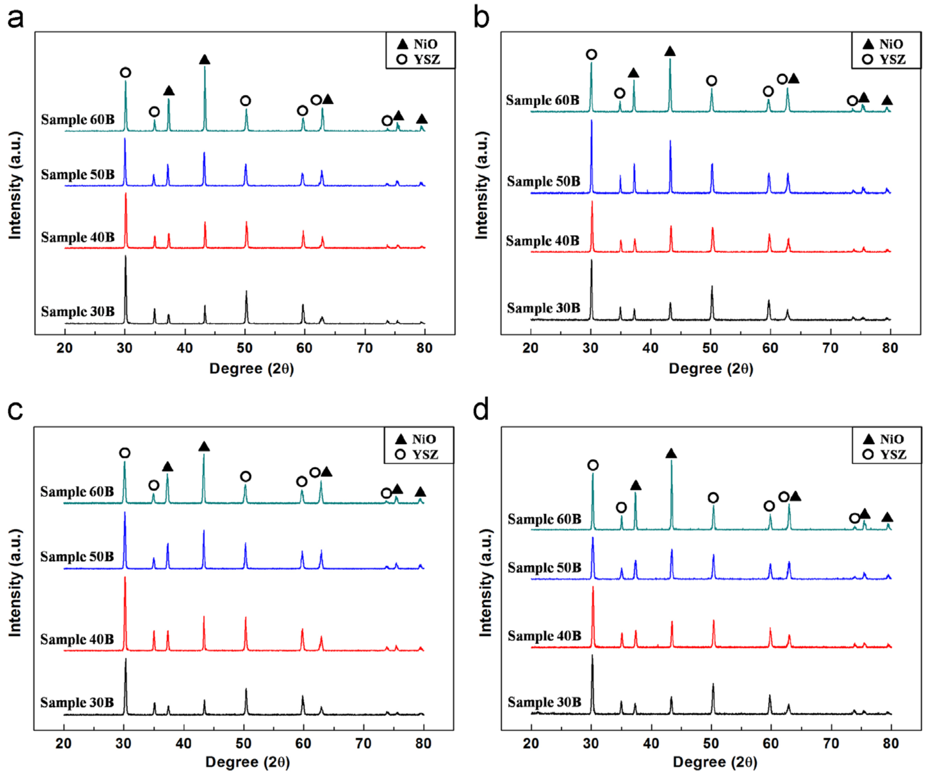

Fig. 1. XRD patterns of the NiO/YSZ composites (5 wt% carbon black) sintered at (a) 1250, (b) 1300 (c) 1350 and (d) 1400 °C.

sintering temperature affect neither the crystal structure nor the phase decomposition. The crystal structure of the sintered NiO/YSZ composites with 10 wt% carbon black was basically the same as that of the sintered NiO/YSZ composites with 5 wt% carbon black (not shown here).

Fig. 2 shows SEM images of the NiO/YSZ composites (5 wt% carbon black) sintered at 1300 °C. It is apparent that distinct grain morphologies and pores can be seen in these figures. It is important to note that the fabricated NiO/YSZ composites exhibit a highly porous structure

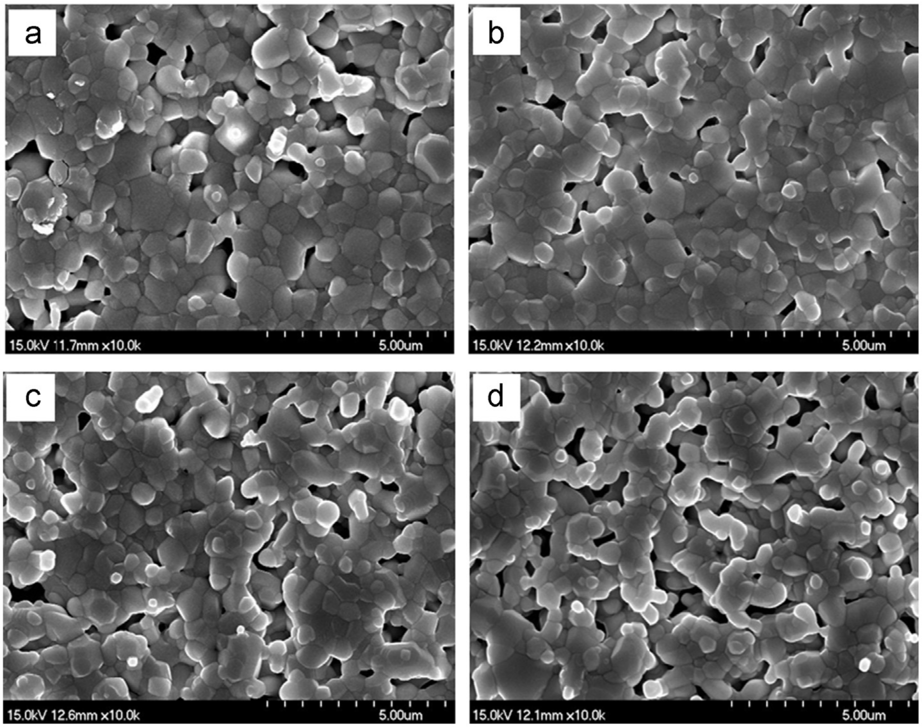

Fig. 2. SEM images of the NiO/YSZ composites (5 wt% carbon black) sintered at 1300 °C: samples (a) 30B, (b) 40B, (c) 50B and (d) 60B.

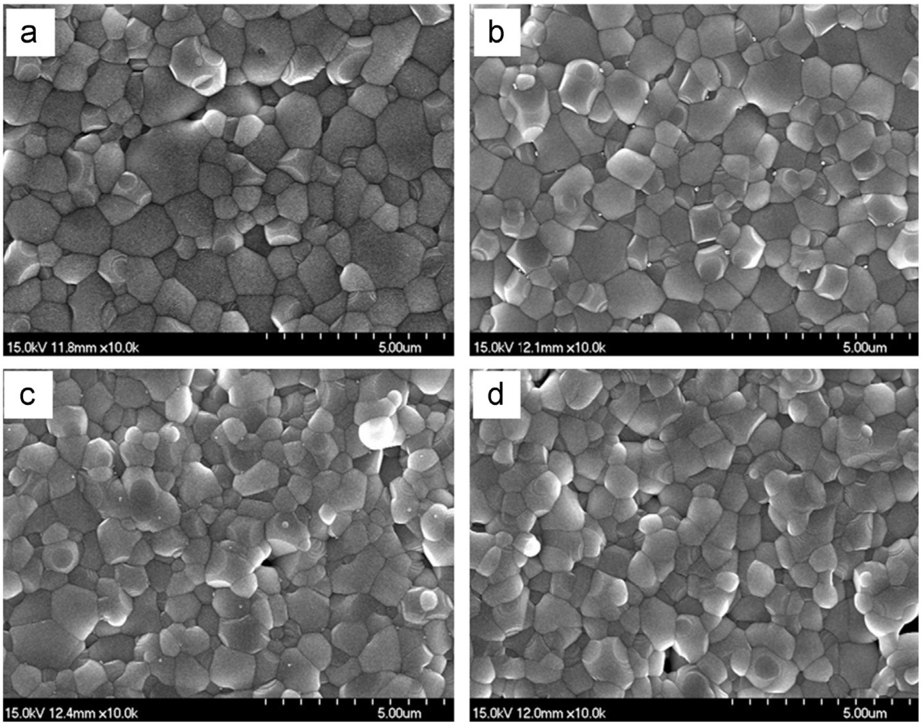

Fig. 3. SEM images of the NiO/YSZ composites (5 wt% carbon black) sintered at 1400 °C: samples (a) 30B, (b) 40B, (c) 50B and (d) 60B.

because of the enhanced evolution of CO and CO_2 gases associated with the following exothermic reactions [16]:

$$\frac{1}{2}C(s)+O_2(g)=CO(g)+110.5\ kJ/mol \qquad (1)$$

$$C(s)+O_2(g)=CO_2(g)+393.5\ kJ/mol \qquad (2)$$

Most pores are located at the grain boundaries. A good contact between the YSZ and NiO grains is achieved during sintering. With a fixed NiO content, the porosity of the composites is notably reduced when the sintering temperature is increased to 1350 and 1400 °C. At the highest sintering temperature (1400 °C), the NiO/YSZ composites

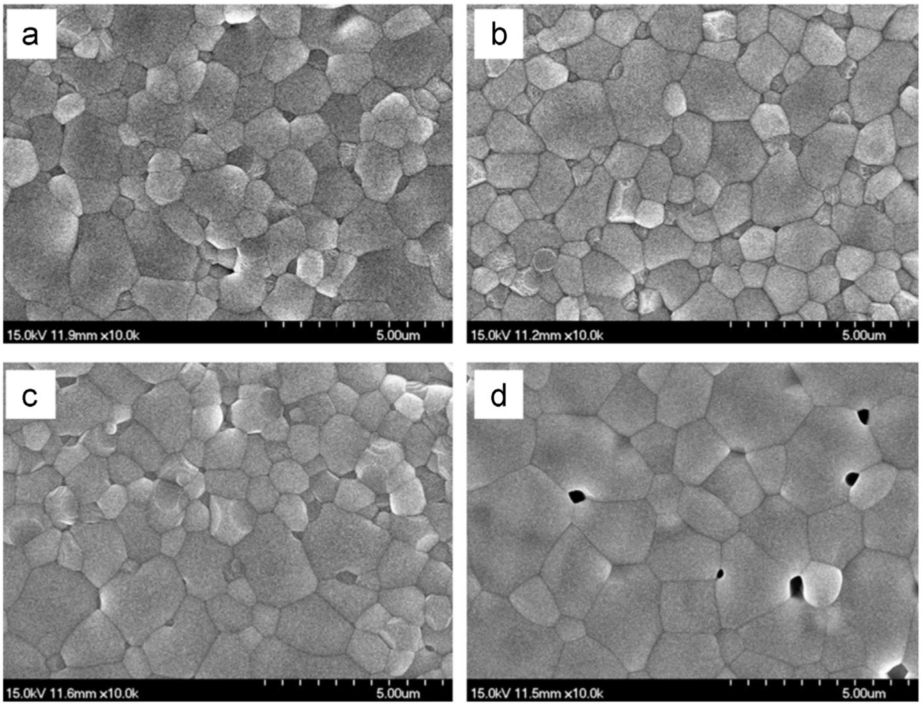

Fig. 4. SEM images of the carbon black-free NiO/YSZ composites sintered at 1400 °C: samples (a) 30A, (b) 40A, (c) 50A and (d) 60A.

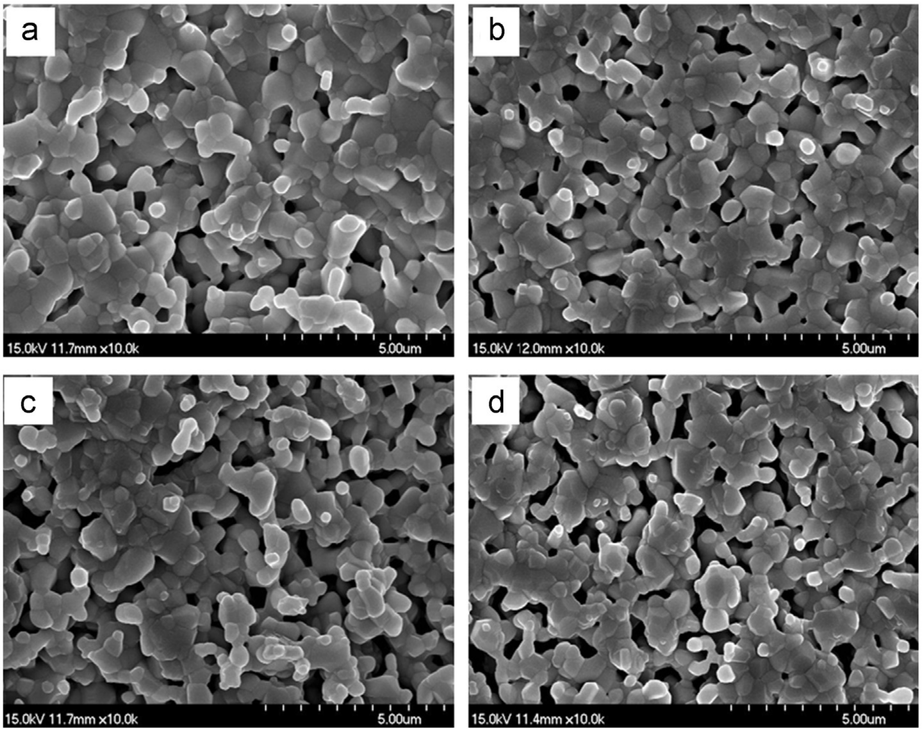

Fig. 5. SEM images of the NiO/YSZ composites (10 wt% carbon black) sintered at 1300 °C: samples (a) 30C, (b) 40C, (c) 50C and (d) 60C.

are fully dense. The SEM images of the NiO/YSZ composites (5 wt% carbon black) sintered at 1400 °C are shown in Fig. 3. The NiO/YSZ composites (5 wt% carbon black) sintered at a low temperature (1250 °C) exhibit a high porosity due to incomplete densification (not shown here).

In addition, the grain size of the composites significantly depends on the added carbon black content. Fig. 4 shows SEM images of the carbon black-free NiO/YSZ composites sintered at 1400 °C. It is also important to note that the average grain size of the carbon black-free composites is larger than that of the carbon black-containing composites. This can be explained by the following two competing effects affecting the grain size: (1) as discussed earlier, the added carbon black generates heat due to exothermic reactions, leading to an increased grain size; and (2) the interaction forces between the added carbon black and grain boundaries exert a dragging effect on the migration of the boundaries, thereby retarding the grain growth. From these competing effects, it is considered that factor (2) dominantly affects the grain size. Similar behavior was found in our previous studies regarding graphite-containing $BaTiO_3$ [18]. The grain size of graphite-containing $BaTiO_3$ was decreased with the graphite content, i.e., 20.1, 16.6, and 10.2 μm for 0.25, 0.75, and 1.25 mol graphite, respectively.

The size of NiO grains is increased with increasing NiO content. This is due to the fact that NiO grains easily grow into larger grain size compared to YSZ grains during the sintering process because the densification temperature of NiO is lower than that of YSZ [17]. Since the solubility of NiO in 8YSZ is very low as discussed previously, the NiO and YSZ grains sinter separately. Furthermore, the porosity of the carbon black-free composites is lower than that of the carbon black-containing composites. This result indicates that the additional porosity is obtained by adding carbon black. At a given sintering temperature, the porosity of the NiO/YSZ composites with 10 wt% carbon black is higher than that with 5 wt% carbon black, which is attributed to the larger evolution of CO and CO_2 gases. This means that the porosity of the NiO/YSZ composites sintered at the same temperature increases when more carbon black is added. SEM images of NiO/YSZ composites with 10 wt% carbon black sintered at 1300 °C are shown in Fig. 5.

The porosities of NiO/YSZ composites with 5 and 10 wt% carbon black, as a function of sintering temperature, are summarized in Fig. 6. This figure shows that the porosity of NiO/YSZ composites sintered at the same temperature tends to increase with NiO content. For example, the porosities of samples 30B, 40B, 50B, and 60B with 5 wt% carbon black sintered at 1300 °C are 13.6%, 15.4%, 20.5%, and 22.6%, respectively. The porosity of the NiO/YSZ composites at the same NiO content is increased with decreasing sintering temperature. For example, the porosities of sample 30B with 5 wt% carbon black sintered at 1250, 1300, 1350, and 1400 °C are 25.1%, 13.6%, 6.9%, and 1.8%, respectively. In addition, at the same NiO content and sintering temperature, the porosities of NiO/YSZ composites with 10 wt% carbon black are much higher than those with 5 wt% carbon black. For example, the porosities of samples 30B and 30C sintered at 1300 °C are 13.6% and 29.6%, respectively.

Fig. 7 shows the XRD patterns of samples 40A, 40B, and 40C reduced at 1000 °C in (Ar + 6% H_2) atmosphere after sintering at 1400 °C. Samples 40A, 40B, and 40C contain the Ni phase with an fcc crystal structure and the YSZ phase with a cubic crystal structure [19,20]. This means that the NiO/YSZ composites are successfully transformed to Ni/YSZ cermets under our reducing condition. There is no significant change in the angle of diffracted peaks of the two phases with carbon black content. Furthermore, when the NiO content in the cermets is increased, the intensity of Ni peaks is increased, whereas the intensity of YSZ peaks is decreased (not shown here). Higher Ni content leads to higher conductivity [9]. Due to the large thermal expansion coefficient mismatch between Ni ($16.9 \times 10^{-6}\ K^{-1}$) and YSZ ($10.8 \times 10^{-6}\ K^{-1}$), a higher amount of Ni in the cermets leads to higher residual stress [9,21].

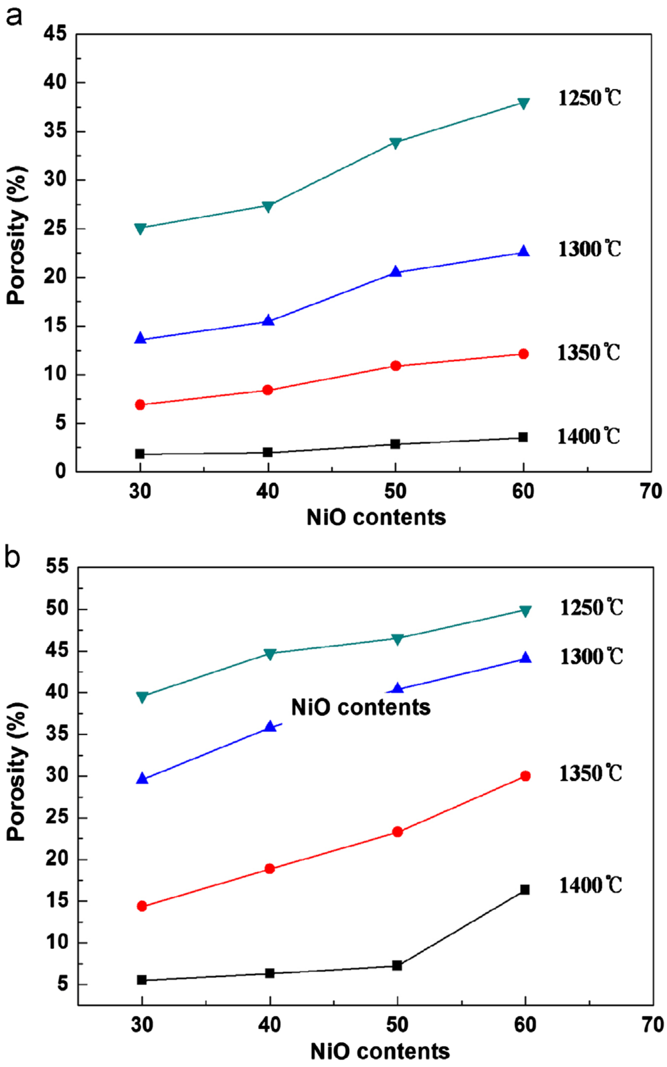

Fig. 6. Porosities of the NiO/YSZ composites with (a) 5 and (b) 10 wt% carbon blacks as a function of sintering temperature.

The electrochemical efficiency depends strongly on the morphology of the Ni/YSZ cermets, which affect the intrinsic catalytic activities and transport properties [22]. Fig. 8 exhibits the surface morphology of the Ni/YSZ cermets (5 wt% carbon black) reduced at 1000 °C in (Ar+6% H_2) atmosphere after sintering at 1300 °C. Highly porous Ni/YSZ cermets are successfully fabricated using porous NiO/YSZ composites. This is attributed to the incomplete densification and gas evolution during sintering as well as oxygen extraction by means of the conversion of NiO to Ni during the reduction treatment [23]. The porous structure can provide sufficient TPB length and can be beneficial for the transport of fuel gas and diffusion of the exhaust gas, thereby promoting the reaction rate [8]. The porosity of the Ni/YSZ cermets is increased by using the NiO/YSZ cermets sintered at low temperature (1250 °C). On the other hand, the samples sintered at high sintering temperatures (1350 and 1400 °C) have lower porosity (not shown here) in comparison with the sample sintered at 1300 °C. We can find a continuous connection of pores, which allows the diffusion of reactants to the active reaction area and the diffusion of reaction products from the active reaction area [11]. The Ni phase provides a pathway for transporting electrons and large catalytic activity for fuel gas to react at the surface of anodes, leading to high electrical conductivity [9,14]. On the other hand, the YSZ phase offers a conductance of oxygen ions and creates interfacial sites with Ni phase for anodic reactions [14].

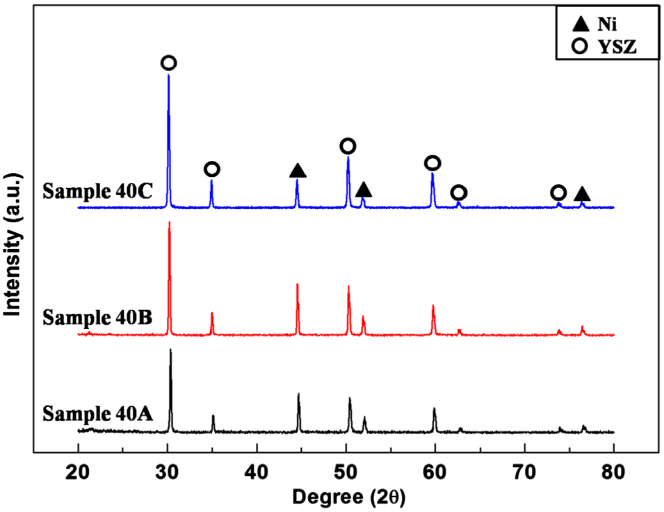

Fig. 7. XRD patterns of the samples 40A, 40B, and 40C reduced at 1000 °C after sintering at 1400 °C.

Table 2 shows the porosities of the Ni/YSZ cermets, considering the NiO content and sintering temperature. The porosity of the cermets is increased after the reduction in (Ar+6% H_2) atmosphere due to the oxygen extraction by means of the change of NiO to Ni [23]. For example, the porosity of sample 40B sintered at 1300 °C is 15.4%, and the porosity of sample 40B sintered at 1300 °C followed by reduced at 1000 °C is 26.6%. The effect of carbon black and NiO content as well as sintering temperature on the porosity of the Ni/YSZ cermets had the same trend as the sintered samples. At a fixed sintering

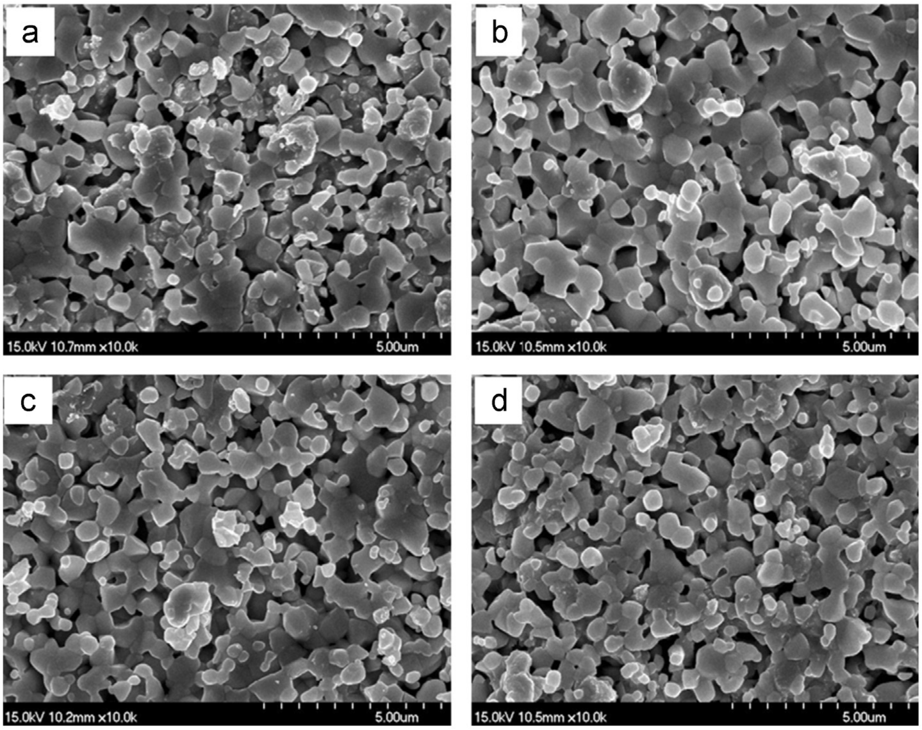

Fig. 8. SEM images of the Ni/YSZ cermets (5 wt% carbon black) reduced at 1000 °C in (Ar+6% H_2) atmosphere after sintering at 1300 °C: samples (a) 30B, (b) 40B, (c) 50B and (d) 60B.

Table 2
Porosities of the Ni/YSZ cermets with 5 and 10 wt% carbon blacks after reduction as functions of composition and sintering temperature.

Sample	Sintering temperature (°C)	Porosity (%)
Sample 30B	1250	34.5
	1300	22.1
	1350	13.3
	1400	6.2
Sample 40B	1250	40.6
	1300	26.6
	1350	17.3
	1400	7.3
Sample 50B	1250	47.2
	1300	36.5
	1350	27.2
	1400	20.9
Sample 60B	1250	52.8
	1300	39.2
	1350	33.2
	1400	24.4
Sample 30C	1250	50.1
	1300	38.5
	1350	18.8
	1400	10.6
Sample 40C	1250	53.1
	1300	40.3
	1350	25.6
	1400	12.1
Sample 50C	1250	55.1
	1300	45.3
	1350	29.4
	1400	19.7
Sample 60C	1250	58.4
	1300	49.6
	1350	39.3
	1400	28.1

temperature of 1300 °C, the porosities of the reduced samples 40B, 40C, 60B, and 60C are 26.6%, 40.3%, 39.2%, and 49.6%, respectively. In addition, the porosities of the reduced sample 40B sintered at 1300 and 1400 °C are 26.6% and 7.3%, respectively. The use of carbon black as a pore-former is a highly effective way to produce porous Ni/YSZ cermets.

4. Conclusions

Porous NiO/YSZ composites were fabricated by the planetary milling of NiO and YSZ powders followed by the sintering of NiO/YSZ green pellets. The carbon black-added NiO/YSZ composites exhibited a highly porous structure because of the enhanced evolution of CO and CO_2 gases during sintering, which was associated with the exothermic reactions during sintering. The addition of carbon black in the NiO and YSZ powders led to a decrease in the density and the grain size of NiO/YSZ composites. At the same NiO content and sintering temperature, the porosity of NiO/YSZ composites with 10 wt% carbon black was much greater than that with 5 wt% carbon black. The porosity of NiO/YSZ composites was increased via decreases in the NiO content and the sintering temperature. The reduction treatment under (Ar+6% H_2) atmosphere led to an increase in the porosity, which was caused by the change of NiO to Ni during the reduction process. The porosity of Ni/YSZ cermets was increased with the NiO content because of the higher porosity of NiO/YSZ composites and the greater extraction of oxygen during the reduction treatment. The use of carbon black as a pore-former was highly effective in producing porous Ni/YSZ cermets.

References

[1] S.A. Acharya, The effect of processing route on sinterability and electrical properties of nano-sized dysprosium-doped ceria, Journal of Power Sources 198 (2012) 105–111.

[2] F. Calise, G. Ferruzzi, L. Vanoli, Parametric energy analysis of a tubular solid oxide fuel cell (SOFC) stack through finite-volume model, Applied Energy 86 (2009) 2401–2410.

[3] M. Yan, M. Zeng, Q. Chen, Q. Wang, Numerical study on carbon deposition of SOFC with unsteady state variation of porosity, Applied Energy 97 (2012) 754–762.

[4] M. Santin, A. Traverso, L. Magistri, Liquid fuel utilization in SOFC hybrid systems, Applied Energy 86 (2009) 2204–2212.

[5] Y.-S. Chou, J.W. Stevenson, P. Singh, Effect of pre-oxidation and environmental aging on the seal strength of a novel high-temperature solid oxide fuel cell (SOFC) sealing glass with metallic interconnect, Journal of Power Sources 184 (2008) 238–244.

[6] L. Jia, Z. Lu, J. Miao, Z. Liu, G. Li, W. Su, Effects of pre-calcined YSZ powders at different temperatures on Ni-YSZ anodes for SOFC, Journal of Alloys and Compounds 414 (2006) 152–157.

[7] J.-Y. Yoo, C.-K. Cho, I.-J. Shon, K.-T. Lee, Preparation of porous Ni-YSZ cermet anodes for solid oxide fuel cells by high frequency induction heated sintering, Materials Letters 65 (2011) 2066–2069.

[8] K. Chen, Z. Lü, X. Chen, N. Ai, X. Huang, B. Wei, J. Hu, W. Su, Characteristics of NiO/YSZ anode based on NiO particles synthesized by the precipitation method, Journal of Alloys and Compounds 454 (2008) 447–453.

[9] S.K. Pratihar, A. Dassharma, H.S. Maiti, Processing microstructure property correlation of porous Ni-YSZ cermets anode for SOFC application, Materials Research Bulletin 40 (2005) 1936–1944.

[10] S.T. Aruna, M. Muthuraman, K.C. Patil, Synthesis and properties of Ni/YSZ cermet: anode material for solid oxide fuel cells, Solid State Ionics 111 (1998) 45–51.

[11] J.J. Haslam, A.-Q. Pham, B.W. Chung, J.F. DiCarlo, R.S. Glass, Effects of the use of pore formers on performance of an anode supported solid oxide fuel cell, Journal of the American Ceramic Society 88 (2005) 512–518.

[12] JCPDS card no. 78-0643.

[13] JCPDS card no. 30-1468.

[14] A. Kuzjukevics, S. Linderoth, Interaction of NiO with yttria-stabilized zirconia, Solid State Ionics 93 (1997) 255–261.

[15] S. Chen, P. Shen, Effect of NiO dissolution on the transformation of plasma-sprayed Y-PSZ, Materials Science and Engineering A 114 (1989) 159–165.

[16] D.R. Gaskell, Introduction to the Thermodynamics of Materials, Taylor & Francis, Washington DC, 1995, pp. 547.

[17] T. Fukui, K. Murata, S. Ohara, H. Abe, M. Naito, K. Nogi, Morphology control of Ni-YSZ cermet anode for lower temperature operation of SOFCs, Journal of Power Sources 125 (2004) 17–21.

[18] K. Park, K.U. Jang, Response characteristics to reducing gases in $BaTiO_3$-based thick films, Journal of Alloys Compounds 391 (2005) 123–128.

[19] JCPDS card no. 04-0850.

[20] JCPDS card no. 82-1246.

[21] M. Mukhopadhyay, J. Mukhopadhyay, A.D. Sharma, R.N. Basu, Ball mill assisted synthesis of Ni-YSZ cermet anode by electroless technique and their characterization, Materials Science and Engineering B 163 (2009) 120–127.

[22] C. Tongxiang, Z. Yanwei, Z. Wei, G. Cuijing, Y. Xiaowei, Synthesis of nanocomposite nickel oxide/yttrium-stabilized zirconia (NiO/YSZ) powders for anodes of solid oxide fuel cells (SOFCs) via microwave-assisted complex-gel auto-combustion, Journal of Power Sources 195 (2010) 1308–1315.

[23] M. Marinsek, K. Zupan, J. Macek, Preparation of Ni-YSZ composite materials for solid oxide fuel cell anodes by the gel-precipitation method, Journal of Power Sources 86 (2000) 383–389.